Mode Switch Assistance to Maximize Human Intent Disambiguation

Author Names Omitted for Anonymous Review. Paper-ID [add your ID here]

***Abstract*—In this paper, we develop an algorithm for mode switch assistance for goal disambiguation with a shared-control assistive robotic arm. Assistive systems are often required to infer human intent and this usually becomes a bottleneck for providing assistance quickly and accurately. We introduce the notion of *inverse legibility* in which the human-generated actions are legible enough for the *robot* to infer the human intent confidently and accurately. The proposed disambiguation paradigm seeks to elicit legible control commands from the human by selecting control modes that maximally disambiguate between the various goals in the scene. We present simulation results which look into the robustness of our algorithm and the impact of the choice of confidence functions on the performance of the system. Our simulation results suggest that the disambiguating control mode computed by our algorithm produces more intuitive results when the confidence function is able to capture the "directedness" towards a goal. We also present a pilot study that explores the efficacy of the algorithm on real hardware. Preliminary results indicate that the assistance paradigm proposed was successful in decreasing task effort (number of mode switches) across interfaces and tasks.**

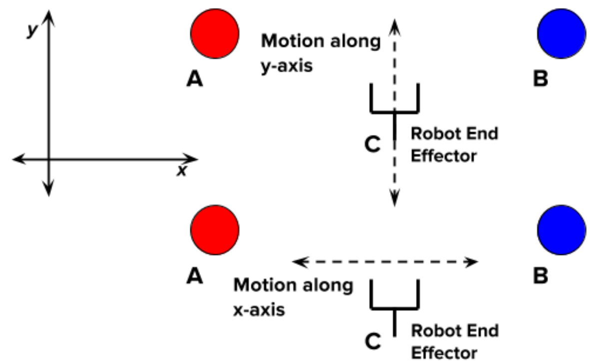

Fig. 1. Illustration of goal disambiguation along various control dimensions. A and B indicate two point goal locations. The robot end effector is at location C. Any motion of the end effector along the y-axis will not help the system to disambiguate between the two goals; that is, the motion is not legible. However, motion along the x-axis allows the goal to be inferred immediately based on the direction in which the robot moves.

I. Introduction

Assistive and rehabilitation devices such as powered wheelchairs, robotic arms and myoelectric prostheses play an important role in the lives of people with motor impairments. These devices help to increase their ability to perform activities of daily lives and reduce their dependence on caretakers, and are crucial to revolutionizing the way they interact with society. As the field of assistive robotics progresses rapidly, the devices themselves become more capable and dextrous—and as a result also more complex, high dimensional and harder to control.

The common paradigm for control of such high-dimensional devices is one has the human directly controls the motion via a control interface. The confounding factor is that the more severe a person's motor impairment, the more limited are the control interfaces available to them to operate. These interfaces (for example, a switch-based head array and Sip-N-Puff) are lower in dimensionality and bandwidth and usually require more mode switches for successful task completion. Thus, a greater need for sophisticated assistive devices is paired with a diminishing ability to control their additional complexity.

Due to the dimensionality mismatch between the control interface and the robotic device, control interfaces operate in *modes* which correspond to different partitions of the control space. Typically, the more limited the control interface is, the greater number of modes there are. In order to have full control of the robot the user will have to switch between the difference partitions of the control space and this is known as *mode switching*.

It has been established that mode switching is expensive and as a result task performance is degraded. Furthermore, it adds to the cognitive and physical burden as each of these mode switches requires the user to shift their attention from the task to performing the mode switch. The introduction of *shared autonomy* to these systems helps to alleviate and address some of these issues by letting the system take responsibility to some extent, thereby reducing the human effort in achieving a goal.

For any assistive autonomy, the system typically needs an idea of what it is the human is trying to do—either by explicit indication of the task or goal [1], or by inferring the human's intent from their control signals and/or sensor data. The question of intent inference is key. In this paper, we develop an assistance paradigm that helps with intent inference, by selecting the control mode in which robot motion will *maximally disambiguate* human intent. In general, the faster the autonomy is able to disambiguate intent, the earlier the robot is able to provide autonomy assistance—leading ideally to fewer mode switches and less burdensome executions.

In many shared-control systems, the assistance provided by the robot is regulated by the robot's ability to estimate user intent confidently and accurately, and it is very unlikely that the robot will be able to determine this with a 100% accuracy. Therefore in the literature to date, the factor dictating how much control lies with the robot versus with the human is usually a function of a confidence metric. This confidence metric is the system's confidence in its own estimate of human intent and is usually a function of the human control command, the autonomous policy, robot pose, goal locations, *et cetera*. This implies that human control actions can potentially have a direct impact on the confidence measure.

The concept of *legibility* is typically used in the domain of Human-Robot Interaction (HRI) as applied to robot motion. A *legible* motion in this context is one which will help the observer (usually the human) decipher the intent behind the robot's action more *quickly* and *confidently*. However, it can be the case that certain actions *by* the human might carry more information than others and better express the human's intent, which can then help the robot to draw useful and correct inferences more easily. Therefore, in this paper we propose a paradigm of *inverse legibility* in which the roles are switched and the human-generated actions *help the robot* to infer human intent confidently and accurately.

Consider the example illustrated in Figure 1. In this example, a human control command issued along the x dimension is more *intent expressive* and helps the robot to provide the right kind of assistance quickly and confidently. With the disambiguation assistance scheme developed in this work, we hope to elicit more legible human control commands by placing the user control in those modes with *maximum disambiguation* between the various goals in the scene.

In Section II we present an overview of relevant research in the area of shared control in assistance systems focusing on mode switching, legibility and synergies in HRI. Section III describes the mathematical formalism for the algorithm and the metric used for goal disambiguation. The empirical methods are outlined in Section IV followed by simulation results in Section V. The pilot study methods, metrics and results are discussed in Section VI, followed by discussion and conlusions in Section VII.

II. RELATED WORKS

Shared-control assistance paradigms help to offload cognitive and physical burden [12] without requiring the user to relinquish complete control, and are usually preferred over fully autonomous assistive robotic systems for reasons of both robustness and user satisfaction. One possible way to control high-dimensional assistive devices such as robotic arms is to partition the control space (often 6D for a robotic arm) into subsets called *modes* and have the user control one mode at a time using control interfaces such as joysticks, head arrays and sip-and-puffs [11, 8]. This is known as *modal control*.

Herlant *et al.* [5] assesses the difficulties faced by users when they operate assistive devices using *modal control*. In their work they report that a significant number of users found *mode switching* to be slow and burdensome. The cognitive burden of shifting focus (*task switching*) from the task at hand to mode switches can result in a significant decrease in task performance regardless of the control modality [7].

A time-optimal mode switch assistance paradigm evaluated on a simulated 2D robot provides insight into the fact that even a simple time-optimal automatic mode switching system can significantly improve user satisfaction while maintaining the quality task performance [5]. Another study [4] found that it is not always the case that users are trying to optimize for time or effort during task execution. However, our present system therefore does not make *a priori* assumptions regarding the optimizing principles at work when a user operates a robot.

Legibility and predictability of robot motion *to the human* have been thoroughly investigated [2], and different methods for generating legible robot motion have been proposed by Holladay *et al* [6]. We apply similar concepts of legibility however to the *human control* commands, such that the intent expressed in the human command is clear *to the robot*. Our assistance scheme is intended to bring out a more legible intent-expressive control command from the human, so that the autonomy is able to infer the correct goal more confidently. As long as the confidence measure used to disambiguate between candidate goals captures the predictable aspect of human-generated robot motion, our proposed disambiguation assistance will place user control in that mode which can provide maximal goal disambiguation and improved legibility.

Also related to our work is the idea of mutual cooperation between humans and robots, and the underlying synergies that are crucial for successful human-robot interaction. The commonplace notion in human-robot interaction, and especially in assistive robotics, is that "help" is provided solely by the robot. In addition to eliciting more legible motion from the human, we also seek to exploit the underlying synergies in human-robot interaction to faciliate more seamless and efficient task execution. From the robot's perspective the key concept behind our algorithm is the idea of *"Help Me, Help You"*—that is, if the human can "help" the robot by providing more legible control commands, then the robot in turn can assist the human even more effectively. This concept has been explored by Goodfellow *et. al* [3] for developing user interfaces that overcome the communication bottleneck that exists between robots and people by accounting for the constrained capabilities of a robot. Sorokin *et al.* [10] proposes a framework for *"people helping robots helping people"* in which humans provide semantic information and judgments about the environment to the robot which then utilizes them to improves its own capabilities. Rosenthal *et al.* [9] proposes a *symbiotic* human robot interaction scheme which aims to overcome perceptual and cognitive limitations that robots might encounter while still allowing the robots to help humans as well.

III. ALGORITHM DESIGN

This section describes the algorithm that is used to compute the control mode with maximum goal disambiguation, thereby eliciting the most legible control command from the human. Section III-A outlines the mathematical notation used in the paper and Section III-B discusses various confidence functions. Section III-C describes the different considerations that inform the confidence disambiguation metric. The details of the underlying shared control system is also described briefly in this Section III-D.

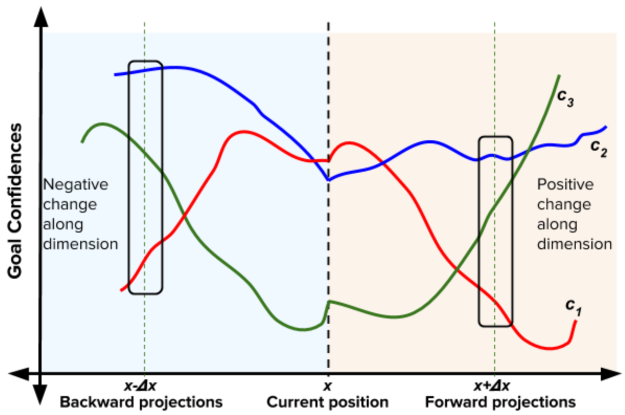

Fig. 2. Illustration of change in confidence with movement along a single control dimension. The region accessible from position x due to positive and negative motion is shaded beige and light blue respectively. Note the discontinuity in the confidences at the current position.

A. Notation

Let $\mathcal{G}$ be the set of all candidate goals in the scene with $n_g = |\mathcal{G}|$ and let g^i refer to the i^{th} goal where $i \in [1, 2, \ldots, n_g]$. The set of goals results in an associated set of confidences denoted as $\mathcal{C}$ where c^i refers to the individual confidence associated with goal g^i. Let $\mathcal{K}$ be the control space in which the robot operates and k^i refer to an individual control dimension where $i \in [1, 2, \ldots, n_k]$. The cardinality of $\mathcal{K}$ depends on the robotic platform; for example, for a smart wheelchair $n_k = 2$ whereas for a 6 DOF robotic arm $n_k = 6$.

For control purposes, the set $\mathcal{K}$ is partitioned into subsets known as *modes*. Let $\mathcal{M}$ refer to the set of all modes that the control space $\mathcal{K}$ is partitioned into with $n_m = |\mathcal{M}|$. The number of modes (n_m) is specific to the control interface and mapping. Furthermore, let m^i refer to the i^{th} mode where $i \in [1, 2, \ldots, n_m]$.

Another quantity of interest is the gradient of individual goal confidences along the different control dimensions. More specifically, $\frac{\partial c}{\partial k}$ captures the rate of change of the confidence c along control dimension k. Furthermore, since the confidence function, in general, can assume drastically different values upon moving in positive and negative directions along a given control dimension, the positive and negative gradients are explicitly denoted as $\frac{\partial c}{\partial k}^+$ and $\frac{\partial c}{\partial k}^-$ respectively. The formalism developed in Section III-C is agnostic to a particular form of confidence function. Additionally, an analytical closed-form expression for the gradient might not always be available as the confidence functions need not be continuous and differentiable. Even when available, due to the complexity of the confidence such an expression might be expensive to compute. Therefore in our work, the gradient is numerically approximated.

We define a *disambiguation* metric, $D_k \in \mathbb{R}$ for each control dimension $k \in \mathcal{K}$, which is a function of c and $\frac{\partial c}{\partial k}$. Analogous to the gradients, we explicitly define disambiguation metrics for both positive and negative motion directions as D_k^+ and D_k^- respectively.

We further define a disambiguation metric $D_m \in \mathbb{R}$ for each control mode $m \in \mathcal{M}$. The disambiguation metric D_m is a measure of how legible the user commands would be if the user were to control the robot in mode m. The higher the value, the easier it will be for the system to infer the human's intent.

B. Confidence function

The choice of confidence function is entirely up to the system designer and numerous options exist. An example of a simple distance-based confidence function is

$$c(\boldsymbol{x}, \boldsymbol{x_g}) = \max(0, 1 - \frac{\|\boldsymbol{x} - \boldsymbol{x}_g\|}{D})$$

where $\boldsymbol{x}$ is the current position of the robot, $\boldsymbol{x}_g$ is the location of goal g and D is the radius of a sphere beyond which the confidence is always 0. We refer to this confidence function as **C1**. However, this confidence measure ignores all cues regarding human intent present in the control command itself. Therefore a better choice of confidence function should try to capture the "directedness" of the human control command towards a goal. One option is

$$c(\boldsymbol{x}, \boldsymbol{x_g}, \boldsymbol{u}_h) = \boldsymbol{u}_h \cdot (\boldsymbol{x}_g - \boldsymbol{x})$$

where $\boldsymbol{u}_h$ is the human control command. We refer to this confidence function as **C2**. **C1** and **C2** can be combined into a single function to capture both "proximity" to and "directedness" towards a goal.

Furthermore, the control signal from the robot autonomy is generated by a function $f_r(\cdot) \in \mathcal{F}_r$,

$$\boldsymbol{u}_r \leftarrow f_r(\boldsymbol{x}) \tag{1}$$

where $\mathcal{F}_r$ is the set of all control behaviors corresponding to different tasks. The algorithm proposed in this paper requires that the confidence measures varies as a function of $\boldsymbol{x}$, so that $\frac{\partial c}{\partial k}$ is well-defined and exists. The specific form of the confidence function and the autonomous robot policy generator will be discussed in Section III-D.

C. Disambiguation metric

Let the component of $\boldsymbol{x}$ along control dimension k be denoted as x_k. Figure 2 is an illustrative example which shows how goal confidences can vary as a function of position along a control dimension.

The disambiguation metric D_k encodes different aspects of how the goal confidences change upon moving (either in the positive or negative direction) along control dimension k. A proper design of D_k should take into account both immediate as well as long term benefits of moving in k and combine them into one metric. We identify four important considerations to inform the design of D_k.

1) Separation in confidences: A good measure for evaluating the confidence disambiguation potential of a control dimension is to compute the *separation* ,SC_k, in goal confidences. At any point in space this can be computed as the *sum of pairwise distances* between the n_g confidences. Since we are interested in the separation after a small change in position (due to user-initiated robot motion), we can sample the confidence function at $x \pm \Delta x$ and use the sampled values to compute SC_k, where Δx is a small change along the control dimension. Thus,

$$SC_k = \sum_{p=1}^{n_g} \sum_{q=p}^{n_g} \left\| c^p_{x_\delta} - c^q_{x_\delta} \right\|$$

where δ indicates $x+\Delta x$ or $x-\Delta x$ depending on the direction of perturbation.

2) Max of confidences: The maximum of the goal confidences is a good measure of the system's overall certainty in accurately estimating human intent. A higher maximum implies that the robot has an even better idea of and is fairly sure of what the human is trying to do. The max (M_k) is computed as

$$M^{\pm}_{k^j} = \max_{1 \le i \le n_g} c^i_{x_j^{\delta \pm}}$$

3) Difference between largest confidences: For the blending paradigm, the current goal ($\boldsymbol{g}^*$) is the one with the highest confidence value. That is,

$$\boldsymbol{g}^* = g^{\operatorname{argmax}_i c^i}$$

Therefore, it is crucial that the difference between the largest and the second largest confidences in $\mathcal{C}$ is significant so that the computation of $\operatorname{argmax}_i c^i$ is likely to generate the current predicted goal. Any ambiguity will likely result in a less accurate prediction of $\boldsymbol{g}^*$. This difference will be denoted by $B^{\pm}_{k^j}$ and is computed as

$$B^{\pm}_{k_j} = \max(\mathcal{C}) - \max(\mathcal{C}^*)$$

where $\mathcal{C}^* = \mathcal{C} \setminus \max(\mathcal{C})$.

4) Gradients: The propensity for change and information gain upon the continuation of motion along control dimension k^j is encoded in the gradients $\frac{\partial c^i}{\partial k^j}$ $\forall$ $c^i \in \mathcal{C}$. The greater the difference between the gradients of individual confidences c^i, the greater will they deviate from each other. Instead of using closed–form analytical gradients, we approximate the gradients using forward and backward differences. Therefore,

$$\frac{\partial c^i}{\partial k^j}^{\pm} \approx c^i_{x_j^{\delta \pm}} - c^i_{x_j}$$

In order to quantify the "spread" of gradients we define a quantity $SD^{\pm}_{k^j}$ which is computed as

$$SD^{\pm}_{k^j} = \sum_{p=1}^{n_g} \sum_{q=p}^{n_g} \left\| \frac{\partial c^p}{\partial k^j}^{\pm} - \frac{\partial c^q}{\partial k^j}^{\pm} \right\|$$

Putting it all together: $SC^{\pm}$, $M^{\pm}$, $B^{\pm}$ and $SD^{\pm}$ are then combined to compute $D^{\pm}_{k^j}$ as

$$D^{\pm}_{k^j} = \underbrace{\boldsymbol{w}_1 (SC^{\pm} \cdot M^{\pm} \cdot B^{\pm})}_{\text{long term}} + \underbrace{(1 - \boldsymbol{w}_1) \cdot SD^{\pm}}_{\text{short term}}$$

where $\boldsymbol{w}_1$ controls the relative contribution of immediate and the long term benefit. Once $D^{\pm}_{k^j}$ is computed D_{k^j} and D_m can be evaluated as

$$D_{k^j} = D^{+}_{k^j} + D^{-}_{k^j}$$

$$D_m = \sum_j D_{k^j} \; \forall \; k^j \in m$$

The control dimension with highest disambiguation capability $\boldsymbol{k}^*$ is given by

$$\boldsymbol{k}^* = \operatorname*{argmax}_j D_{k^j}$$

and the mode with highest disambiguation capability $\boldsymbol{m}^*$ is given by

$$\boldsymbol{m}^* = \operatorname*{argmax}_m D_m$$

$\boldsymbol{m}^*$ is the mode that the algorithm chooses *for* the human upon assistance request. Any subsequent control command issued by the user in $\boldsymbol{m}^*$ is likely to the more legible due to maximal goal confidence disambiguation.

D. Blending paradigm

The proposed mode switching assistance paradigm augments a blending based shared control system in which the final control command issued to the robot is a blended sum of the human control command and an autonomous robot policy. The blending factor (α) is a function of the system confidence in its own estimate of the human intent.

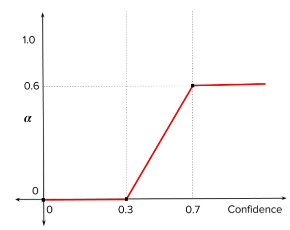

Fig. 3. A prototypical arbitration function.

Let $\boldsymbol{u}^i_r$ be the autonomous control policy associated with goal g^i. The final control command $\boldsymbol{u}$, issued to the robot is then given as

$$\boldsymbol{u} = \alpha \cdot \boldsymbol{u}^{i^*}_r + (1 - \alpha) \cdot \boldsymbol{u}_h$$

where i^* is the index associated with $\boldsymbol{g}^*$.

The robot control command $\boldsymbol{u}^i_r$ is generated using a simple potential field based dynamical system which is defined in all parts of the state space. Every goal g^i is associated with a potential field P^i which treats g^i as an attractor and all the other goals in the scene as repellers. For potential field P^i, the attractor velocity is given by

$$\dot{\boldsymbol{x}}^i_{attract} = \boldsymbol{x}_{g^i} - \boldsymbol{x}$$

where $\boldsymbol{x}_{g^i}$ is the location of g^i and the repeller velocity

$$\dot{\boldsymbol{x}}^i_{repel} = \sum_p \frac{\boldsymbol{x} - \boldsymbol{x}_{g^p}}{\eta(\|\boldsymbol{x} - \boldsymbol{x}_{g^p}\|^2)}$$

where $p \in \{1, 2, \ldots, n_g\} \setminus \{i\}$ and $\dot{\boldsymbol{x}}$ indicates the velocity of the robot in the world frame. Therefore,

$$\boldsymbol{u}_r^i = \dot{\boldsymbol{x}}_{attract}^i + \dot{\boldsymbol{x}}_{repel}^i$$

Additionally, P^i operates in full six dimensional Cartesian space and treats position and orientation as independent potential fields.

In our implementation c^i is computed as

$$c^i(\boldsymbol{x}, \boldsymbol{u}_h, \boldsymbol{u}_r^i) = \boldsymbol{u}_h^{trans} \cdot (\boldsymbol{x}_{g^i} - \boldsymbol{x})^{trans} + \boldsymbol{u}_h^{rot} \cdot \boldsymbol{u}_r^{i(rot)} \quad (2)$$

where $trans$ refers to the translational and rot refers to the rotational parts of the entire control space. The first term captures the "directedness" of the human control command towards the goal g^i and the second term captures the alignment between the human control command and the autonomous robot policy in the rotational parts of the state space respectively. The blending factor α is a parameterized function of the confidence and is depicted in Figure 3.

IV. EMPIRICAL VALIDATION

A. Hardware

1) Robotic Platform: The experiments were performed using the MICO robotic arm (Kinova Robotics, Canada) which is a 6 DOF robotic arm specifically designed for assistive purposes. The software system was implemented using the Robot Operating System (ROS) and data analysis was performed using MATLAB.

B. Assistance Paradigms

Three kinds of mode switching assistance paradigms were tested in this pilot study. Note that the blending assistance was always running for all three paradigms.

Manual: In this paradigm the user manually performs all mode switches. The starting control mode is randomized.

Assisted: In this paradigm, the mode switch system is activated right at the beginning of a trial. The algorithm identifies the "best mode" $\boldsymbol{m}^*$ and starts the trial in control mode $\boldsymbol{m}^*$. All subsequent mode switches are performed manually by the user. Furthermore, the user was required to first move in the selected mode before manually switching the mode.

On Demand: In this paradigm, the user can request a mode switch assistance at any time during task execution. This paradigm is exploratory and seeks to find underlying patterns in assistance request behavior.

V. SIMULATION RESULTS

Choice of confidence functions: Since D_{k^j} and D_{cm} are evaluated using c^i and $\frac{\partial c^i}{\partial k^j}$, they are both indirectly functions of $\boldsymbol{x}$. The choice of confidence functions can also greatly affect the computation of $\boldsymbol{k}^*$ and $\boldsymbol{m}^*$. In order to quantify the differences between different choices for confidence functions, we performed simulations in which $\boldsymbol{k}^*$ was computed at 2000 uniformly sampled points in the workspace of the robot, approximated as a $1.2 \times 0.6 \times 0.7m^3$ volume in front of the robot. **C1** and **C2** were chosen as the confidence functions and the goals were the same as in *RsG*.

Figure 6 shows the results of the simulation and it can be clearly seen that the choice of confidence functions changes the preferred control dimensions in the workspace quite significantly. More importantly, it also sheds light on the efficacy of a confidence function to capture human intent properly. For the goal distribution used in the simulation the goal positions are spread out maximally along the x and z axes. Intuitively the system will be able to quickly infer the human's intent if the human control command is either along the x or the z axes. However, this requires that the confidence function indeed captures the "directedness" of the human control command. Table I reports the number of times the algorithm picked each of the three control dimensions for each confidence function. It is clear that **C1** was not be able to capture the human intent properly as seen in Table I. Furthermore, **C1** had "null" spaces where all confidences were identically equal to zero and therefore disambiguation was not possible. On the other hand with **C2**, the algorithm identified x as the preferred dimension 1711 out of 2000 samples which indicates that the confidence function along with the algorithm was able to generate the most intuitive and useful dimension nearly 86% of the time and the second preferred dimension was z. The algorithm picked y only when the robot directly in front of a goal.

Best control dimension distribution				
Confidence Function	**X**	**Y**	**Z**	**NULL**
C1	579	615	446	360
C2	1711	93	196	0

TABLE I
BEST CONTROL DIMENSION DISTRIBUTION FOR TWO DIFFERENT CONFIDENCE FUNCTIONS.

Characterization of control mode: In our algorithm, the computation of D_m is simplified and *only* considers projected motion along $k_j \in m$. However, in reality the user can generate any arbitrary control command in a control mode which can potentially cause the robot along any vector spanned by the control dimensions in m. This can alter the computed disambiguation capability of being in $\boldsymbol{m}^*$. In order to test whether the simplification was indeed sufficient to characterize the disambiguation capability of being in a mode, we performed simulations in which $\boldsymbol{m}^*$ was computed for 500 uniformly sampled locations in the robot workspace. At each of those points, 100 random control commands that are feasible in $\boldsymbol{m}^*$ were generated and applied to the robot which resulted in change in positions. Finally, at each of these "perturbed" positions the best control mode was once again computed and if this matched with $\boldsymbol{m}^*$ it indicates that algorithm is robust enough and the simplification was sufficient for characterizing the mode completely. Table II summarizes the number of times the match occurred (in percentage) for different number of goals. We also observed that as the number of goals increased the accuracy dropped. Intuitively this makes sense because disambiguation between goals will become harder as the number of goals increase.

Fig. 4. Pilot study tasks performed by the subjects. *Left to right:* Simple Reaching (*Rp*), Reaching with same grasp (*RsG*), Reaching with different grasp (*RdS*).

Match percentage	
n_g	**Accuracy%**
3	90.06
4	86.86
5	85.65

TABLE II
ACCURACY FOR ???

Control Mappings		
Mode	**HA**	**J2**
1	v_x	v_x, v_y
2	v_y	v_x, v_z
3	v_z	ω_z, ω_y
4	ω_z	ω_x
5	ω_y	—
6	ω_x	—

TABLE III
OPERATIONAL PARADIGMS FOR THE TELEOPERATION INTERFACES

VI. PILOT STUDY

1) Control Interfaces: In our experiments, the human control command $\boldsymbol{u}_h$ was captured using two different control interfaces: 2-axis joystick (J2) and a head array (HA) shown in Figure 5. J2 generates continuous signals and is capable of controlling a maximum of two control dimensions at a time. Control modes can be accessed using the buttons on the interface. On the other hand, HA is a switch–based discrete teleoperation device. HA consists of three switches; the switch at the back is used to cycle between the modes and the switches on the left and right side are to control the motion in the positive and negative direction along a control dimension.

Fig. 5. 2-axis joystick (left) and switch–based head array (right)

The control interface signals are mapped to Cartesian velocities of the end effector of the robot (Table III). Additionally, the interfaces can also be used to request mode switch assistance.

A. Task Descriptions

Three tasks were developed for our pilot study (Figure 4).
Simple Reaching (Rp) : The user operates the robotic arm using both control interfaces to perform simple reaching motions to three different goal locations. This is a training task and the primary purpose is to get the user accustomed to the operation of the control interfaces, the underlying blending based assistance and the experiment protocol.
Reaching with same grasp (RsG) : The user teleoperates the robotic arm using both control interfaces to perform reaching motions towards one of the four objects on the table with the same grasp orientation.
Reaching with different grasp (RdG): This is a more difficult task that *RsG* in which the user operates the robot to perform reaching motions to one of the five objects in the scene with different grasp orientations.

Analysis was performed only on data collected from *RsG* and *RdG*.

B. Pilot Study Protocol and Metrics

Subjects: For this pilot study 4 able-bodied lab members were recruited (3 males and 1 female).
Protocol: A within-subject study was conducted using a full factorial design in which the manipulated variables are the tasks, control interfaces and assistance paradigms. Each task consisted of two phases.

In phase I, each user performed the task using both interfaces under *manual* and *assisted* paradigms. The trials were balanced and the control interfaces and the paradigms were randomized to eliminate ordering effects. The starting positions of the robot were also randomized to avoid biases. Three trials were collected for each permutation of manipulated variables. In phase II, the user performed the same task using

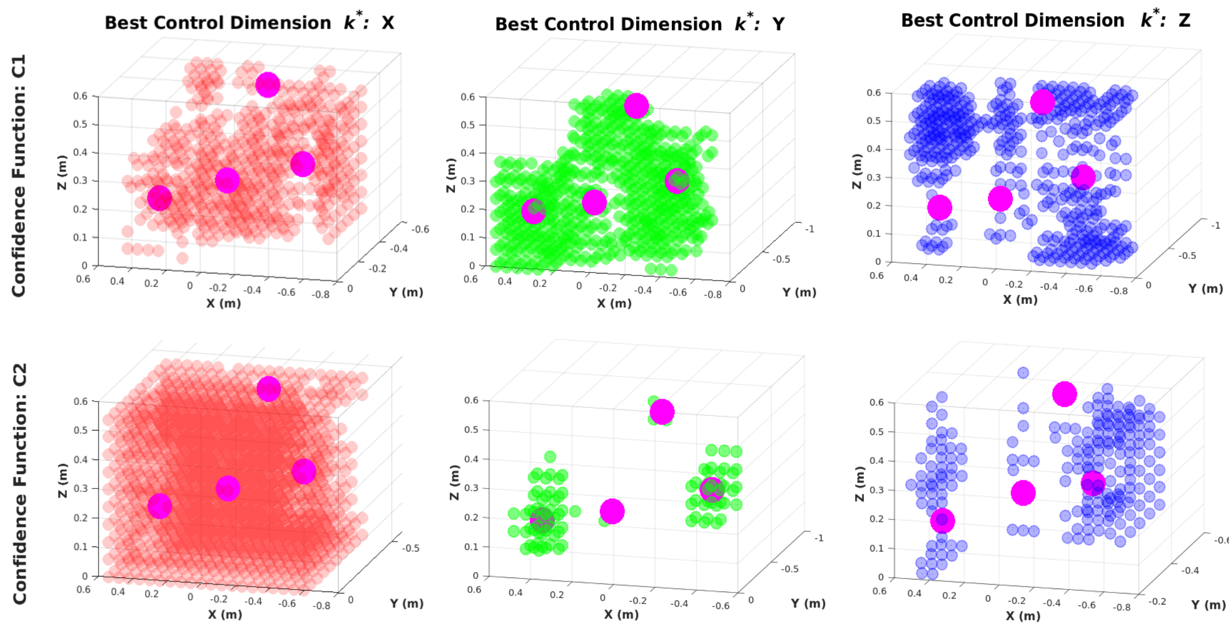

Fig. 6. Top row: Best control dimensions for confidence measure from Equation III-B. Bottom row: Best control dimensions for confidence measure from Equation III-B. Left column: $\boldsymbol{k}^*$ is X. Middle Column: $\boldsymbol{k}^*$ is Y and Right Column: $\boldsymbol{k}^*$ is Z. Magenta spheres indicate the goal locations.

both interfaces using the *on-demand* paradigm and two trials were collected for each task-interface combination.

Metrics: A number of objective metrics were evaluated during this pilot study. *Task completion time* is the amount of time a user spends in accomplishing a task. *Mode switches* refer to the number of times the user switched between various modes while performing the task and is an indicator of effort.

C. Pilot Study Results

Here we report the preliminary results of our pilot study. An improvement in task performance in terms of a decrease in the number of mode switches was observed across all task–interface combinations. Statistical significance in Figure 7 is determined by two-sided Wilcoxon Rank-Sum Test, where (*) indicates $p < 0.05$.

Mode Switches: Figure 7 (top row) reveals the general trend of a decrease in the number of mode switches across all task–interface combinations. However, the difference in the number of mode switches was statistically significant only for *RsG*–joystick (p = 0.014) and *RdG*–joystick (p = 0.024) combination. This indicates that upon starting in a mode identified by the algorithm, the number of subsequent mode switches performed by the user was reduced. This is likely because, the initial mode picked by the algorithm would have the let the user navigate to *any* of the goals easily and at the same time provide more legible commands to the robot.

Task Completion Time: In Figure 7 (bottom row), a decrease in task completion times during *assisted* paradigm was observed in all but one case: *RdG*–headarray combination. However, these differences were not statistically significant for any of the task–interface combinations. The anomalous case of an increase in task completion time for *RdG*–headarray combi-

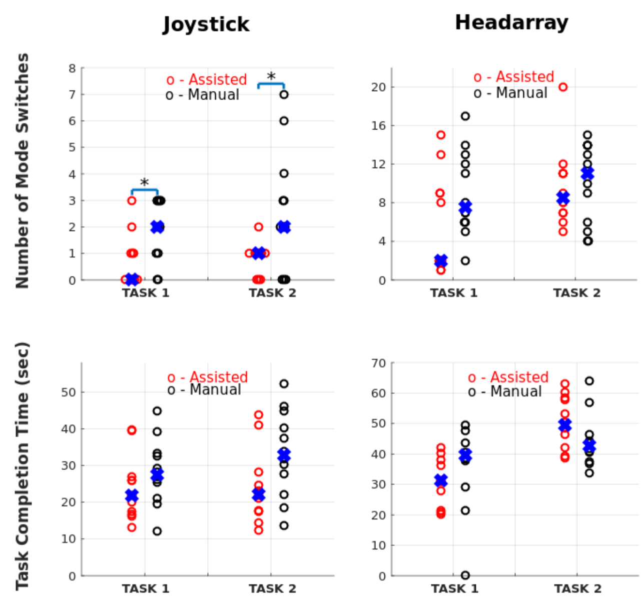

Fig. 7. Top row: Number of Mode switches for joystick (left) and head array (right) for Assisted vs. Manual paradigms. Bottom row: Task Completion Times for joystick (left) and head array (right) for Assisted vs. Manual paradigms.

nation can be explained by the fact that a *single* mode switch assistance at the beginning of the trial probably did not make a huge difference as the task required multiple mode switches to operate in the orientation space as well and thereby would have resulted in an increase in task completion time.

On–Demand: The number of assistance requests for each task–interface combinations is reported in Table IV. The subjects

	J2		HA	
SubID	*RsG*	*RdG*	*RsG*	*RdG*
H1	1	0	5	6
H2	1	1	3	6
H3	2	2	4	5
H4	2	5	17	7

TABLE IV
TOTAL NUMBER OF ASSISTANCE REQUESTS DURING ON-DEMAND PARADIGM.

demonstrated a wide range of assistance request behaviors. Some of the users were more timid in requesting assistance and preferred to perform the task on their own, whereas others were curious enough to explore the on–demand option and operate in the mode assigned by the system.

VII. DISCUSSION AND CONCLUSIONS

Our simulation results indicate that the choice of confidence function has a huge impact on the performance of our algorithm. Confidence functions that encode the "directedness" present in the human control command is likely to be more effective in capturing human intent. Currently the algorithm assumes that at any point in the workspace all the goals in the scene are equally likely. However, in the real scenario, the user usually has an idea of what goal s/he is going for. Therefore, it might be useful to bias the computation of the "best control mode" by looking for cues in the past history of the robot trajectory and control commands such that the control mode chosen will always be useful for the human in reaching the goal s/he has in mind. This will also likely improve the robustness and result in higher user acceptance. Secondly, the algorithm only tries to maximize the utility value *for* the robot. Concepts from decision theory can be used to augment the current framework to also include a utility function *for* the human. Lastly, the algorithm can be used to pre-compute the best modes ahead of time and can be used as a look-up table during task execution for automated mode switching. A single mode switch assistance provided at the beginning of the trial might not be enough to and therefore automated mode switching during task execution will be critical to improve task performance especially for more limited interfaces.

In this paper, we developed an algorithm for mode switch assistance that augments an underlying blending-based shared control system for an assistive robotic arm. We also introduced the notion of *inverse legibility* in which the human generated actions are legible enough *for* the robot to infer the human intent confidently and accurately. The goal of the algorithm developed in this paper is to seek legible control commands from the human by placing the control in those modes with *maximum confidence disambiguation* between the various goals in the scene. A within subject pilot study was designed to test the proposed algorithm. Preliminary results indicated that the assistance paradigm proposed was successful in decreasing task effort (number of mode switches) across interfaces and tasks. Numerous simulation results were also presented which tested the robustness of the algorithm and the impact of different confidence functions on the results.

ACKNOWLEDGMENTS

Funding source omitted for review.

REFERENCES

[1] Young Sang Choi, Cressel D Anderson, Jonathan D Glass, and Charles C Kemp. Laser pointers and a touch screen: intuitive interfaces for autonomous mobile manipulation for the motor impaired. In *Proceedings of the 10th international ACM SIGACCESS conference on Computers and accessibility*, pages 225–232. ACM, 2008.

[2] Anca D Dragan, Kenton CT Lee, and Siddhartha S Srinivasa. Legibility and predictability of robot motion. In *2013 8th ACM/IEEE International Conference on Human-Robot Interaction (HRI)*, pages 301–308. IEEE, 2013.

[3] Ian J Goodfellow, Nate Koenig, Marius Muja, Caroline Pantofaru, Alexander Sorokin, and Leila Takayama. Help me help you: Interfaces for personal robots. In *Proceedings of the 5th ACM/IEEE international conference on Human-robot interaction*, pages 187–188. IEEE Press, 2010.

[4] Deepak Gopinath, Siddarth Jain, and Brenna D Argall. Human-in-the-loop optimization of shared autonomy in assistive robotics. *IEEE Robotics and Automation Letters*, 2(1):247–254, 2017.

[5] Laura V Herlant, Rachel M Holladay, and Siddhartha S Srinivasa. Assistive teleoperation of robot arms via automatic time-optimal mode switching. In *The Eleventh ACM/IEEE International Conference on Human–Robot Interaction (HRI)*, pages 35–42. IEEE, 2016.

[6] Rachel M Holladay, Anca D Dragan, and Siddhartha S Srinivasa. Legible robot pointing. In *The 23rd IEEE International Symposium on Robot and Human Interactive Communication (RO-MAN), 2014*, pages 217–223. IEEE, 2014.

[7] Stephen Monsell. Task switching. *Trends in cognitive sciences*, 7(3):134–140, 2003.

[8] Marnix Nuttin, Dirk Vanhooydonck, Eric Demeester, and Hendrik Van Brussel. Selection of suitable human-robot interaction techniques for intelligent wheelchairs. In *Robot and Human Interactive Communication, 2002. Proceedings. 11th IEEE International Workshop on*, pages 146–151. IEEE, 2002.

[9] Stephanie Rosenthal, Joydeep Biswas, and Manuela Veloso. An effective personal mobile robot agent through symbiotic human-robot interaction. In *Proceedings of the 9th International Conference on Autonomous Agents and Multiagent Systems*, pages 915–922. International Foundation for Autonomous Agents and Multiagent Systems, 2010.

[10] Alexander Sorokin, Dmitry Berenson, Siddhartha S Srinivasa, and Martial Hebert. People helping robots helping people: Crowdsourcing for grasping novel objects. In *2010 IEEE/RSJ International Conference on Intelligent Robots and Systems (IROS)*, pages 2117–2122. IEEE, 2010.

[11] Katherine Tsui, Holly Yanco, David Kontak, and Linda Beliveau. Development and evaluation of a flexible interface for a wheelchair mounted robotic arm. In *Proceedings of the 3rd ACM/IEEE international conference on Human robot interaction*, pages 105–112. ACM, 2008.

[12] Ivan Volosyak, Oleg Ivlev, and Axel Graser. Rehabilitation robot friend ii-the general concept and current implementation. In *9th International Conference on Rehabilitation Robotics (ICORR), 2005*, pages 540–544. IEEE, 2005.